Pippard Relation Modified for the Rotatory Lattice Mode in Ammonia Solid II

H.Yurtseven

Department of Physics,
Middle East Technical University,
Ankara 06531-Turkey
e-mail: hamit@metu.edu.tr

(Received May 25, 2005: final form July 28, 2005)

ABSTRACT

In this study we obtain a linear variation of the specific heat Cp with the Raman frequency shifts $\frac{1}{\nu}(\frac{\partial \nu}{\partial T})_P$ for the rotatory lattice (librational) mode in the ammonia solid II near the melting point. From this linearity, we deduce values of the slope dP_m/dT for the pressures of 3.65, 5.02 and 6.57 kbars in the ammonia solid II. Our calculated value of dP_m/dT for the pressure of 3.65 kbar, is in good agreement with the experimentally measured value in the $P-T$ phase diagram of this crystalline system. This indicates that the first Pippard relation modified for the rotatory lattice mode in the ammonia solid II, is satisfactory near the melting point.

Key words: Pippard relation, ammonia solid II, lattice mode, melting point.

1. INTRODUCTION

Ammonia has been attractive to study, in particular near the melting point. Since it exhibits various phases including a mixture of solid and liquid phases in the $V - T$ phase diagram /1/ and the three solid phases, namely, solid I, II and III phases in the $P - T$ phase diagrams /2-4/, many physical properties can be studied experimentally and theoretically in this system. On the basis of the $P - T$ phase diagrams /2,4/, we have calculated using the mean field theory $P - T$ phase diagrams in the ammonia solid I-II /5/ and solid I,II and III /6/ phases near the melting point.

In the first studies on ammonia in earlier years, measurements of the specific heat /7/, densities /8/ and also the thermal expansion /9/ of ammonia were performed experimentally.

Regarding the crystal structures of the solid ammonia, x-ray /10/ and the neutron scattering /11/ techniques have been used, and it has been reported that the ammonia solid I has a cubic structure with two molecules per unit cell. Also, the experimental techniques have determined a face-centered cubic structure with four molecules per unit cell in ammonia solid II /12/. Another solid phase, ammonia solid III, which has been discovered experimentally at 25^{0}C at a high pressure of 35 kbar /2/, has a hexagonal closed-packed structure. In regard to this structural analysis, the Raman measurements have concentrated on the lattice modes in the ammonia solid I /1,3/ and solid II /3,13,14/. The thermodynamic properties have also been studied; in particular, the volumetric measurements as a function of pressure have been performed for the ammonia solid I and solid II near the melting point /15,16/. Using these volumetric data /15,16/ and the Raman data /I/, we have calculated the Raman frequencies of lattice modes as functions of temperature /17/ and of pressure /18/ in the ammonia solid I. Recently, we have calculated the Raman frequencies of

the rotatory lattice (librational) mode in the ammonia solid II as a function of temperature for the fixed pressures of 3.67, 5.02 and 6.57 kbars /19/. We have also been able to calculate the Raman frequencies of this phonon mode at various pressures for some fixed temperatures of 230.4 K, 263.4K and 297.5K in ammonia solid II /20/.

The Pippard relations can be established for the solid structures of ammonia near the melting point. This has been considered partly in some previous studies /15,16/. We have studied two Pippard relations, namely, a linear variation of the specific heat C_p with the thermal expansivity α_P (first Pippard relation) and also a linear variation of α_P with the isothermal compressibility κ_T (second Pippard relation) near the melting point for both ammonia solid I and II in our earlier study /21/.

Spectroscopically, the Pippard relations can be modified using the frequency shifts $\frac{1}{\nu}(\frac{\partial \nu}{\partial T})_P$ or $\frac{1}{\nu}(\frac{\partial \nu}{\partial P})_T$ by means of the mode Grüneisen parameter which can be taken as a constant near the melting point in ammonia. As we have modified the Pippard relations using the Raman frequency shifts of the phonon modes in the ammonium halides near the λ-point /22/, we should be able to modify the Pippard relations using the solid structures of ammonia near the melting point. For this, we choose the rotatory lattice (librational) mode in ammonia solid II near the melting point, on the basis of our earlier work /19/. By means of the Raman frequency shifts which we calculated for this rotatory lattice mode, we establish a linear variation of the specific heat C_p with the frequency shifts $\frac{1}{\nu}(\frac{\partial \nu}{\partial T})_P$ near the melting point in ammonia solid II. We establish this linearity between C_p and $\frac{1}{\nu}(\frac{\partial \nu}{\partial T})_P$ for three fixed pressures of 3.67, 5.02 and 6.57 kbars in the ammonia solid II.

2. THEORY

The thermodynamic quantities such as the specific heat, thermal expansivity and the isothermal compressibility can be studied near the melting point in ammonia solid II. This critical behaviour near the melting point can be expressed as a power-law, starting with the isothermal compressibility κ_T

$$\kappa_T = k(P - P_m)^{-\gamma} \tag{2.1}$$

This is the pressure dependence of κ_T near the melting pressure P_m, γ is the critical exponent and k is the amplitude for ammonia. Using the definition of the isothermal compressibility $\kappa_T = -\frac{1}{V}(\frac{\partial V}{\partial P})_T$, the solid volume in ammonia can be expressed as

$$V_s = V_c \exp[-k(1-\gamma)^{-1}(P - P_m)^{1-\gamma}] \tag{2.2}$$

which has been given previously by Pruzan et al. /16/. In Eq.(2.2) V_c is the critical volume.

From this pressure dependence of the solid volume V_s, its temperature dependence can be obtained for fixed pressures by considering the slope definition

$$\frac{P - P_m(T)}{T_m(P) - T} = \frac{dP_m}{dT} \tag{2.3}$$

near the melting point in ammonia solid II.

This has also been considered in some detail in previous studies /15,23/. Thus, the temperature dependence of the isothermal compressibility, using Eq. (2.3) in Eq. (2.1), becomes

$$\kappa_T = k(\frac{dP_m}{dT})^{-\gamma}[\ T_m(P) - T\ ]^{-\gamma} \tag{2.4}$$

and the solid volume will then become by means of Eq.(2.3),

$$V_s = V_c \exp[-k(1-\gamma)^{-1}(\frac{dP_m}{dT})^{1-\gamma}(T_m - T)^{1-\gamma}] \tag{2.5}$$

The thermal expansivity α_P and the specific heat C_p can also be expressed as functions of pressure and temperature. Using the thermodynamic relation

$$\frac{\alpha_P}{\kappa_T} = (\frac{dP_m}{dT}) = V_c^{-1}\kappa_T^{-1}(\frac{dV_c}{dT}) \tag{2.6}$$

the pressure and the temperature dependence of α_P will

be written, respectively, as

$$\alpha_p = k(\frac{dP_m}{dT})\ (P-P_m)^{-\gamma} + \frac{1}{V_c}(\frac{dV_c}{dT}) \qquad (2.7)$$

and

$$\alpha_p = k(\frac{dP_m}{dT})^{1-\gamma}(T_m - T)^{-\gamma} + \frac{1}{V_c}(\frac{dV_c}{dT}) \qquad (2.8)$$

near the melting point in ammonia solid II.

Finally, the pressure and temperature dependence of the specific heat C_p can be obtained using the thermodynamic relation

$$C_P - C_V - TV\frac{\alpha_P^2}{\kappa_T} \qquad (2.9)$$

where $C_V = T(\partial S/\partial T)_V$. In our earlier study we have derived the temperature and pressure dependence of κ_T, α_P and C_p using the volume expressions (Eqs. 2.2 and 2.5) for ammonia solid I and II near the melting point /23/.

The Raman frequencies can be calculated using the crystal volume by means of the mode Grüneisen parameter for ammonia solid II near the melting point. Since the Grüneisen parameter measures the volume dependence of the frequency, defined as

$$\gamma_P = -\frac{1}{\alpha_P}\frac{1}{\nu}(\frac{\partial \nu}{\partial T})_P \qquad (2.10)$$

with the thermal expansivity $\alpha_P \equiv \frac{1}{V}(\frac{\partial V}{\partial T})_P$, the Raman frequency can be evaluated as

$$\nu_P(T) = A(P) + \nu_m \exp[-\gamma_P \ln\frac{V_P(T)}{V_m}] \qquad (2.11)$$

for ammonia solid II near the melting point. γ_P represents the isobaric mode Grüneisen parameter, V_m and ν_m are the volume and the Raman frequency at the melting point. In Eq.(2.11) the pressure-dependent term $A(P)$ can be written as

$$A(P) = a_0 + a_1 P + a_2 P^2 \qquad (2.12)$$

with the constant parameters a_0, a_1 and a_2.

We have already given the frequency expression (Eq. 2.11) to calculate the Raman frequency of the rotatory lattice (librational) mode in the ammonia solid II near the melting point in our earlier work /19/. Once the Raman frequencies are determined by Eq.(2.11), the Raman frequency shifts $\frac{1}{\nu}(\frac{\partial \nu}{\partial T})_P$ can be evaluated for the ammonia solid II near the melting point. These frequency shifts can be related to the thermodynamic quantities such as the specific heat C_p, the thermal expansivity α_P and the isothermal compressibility κ_T for the ammonia solid II near the melting point. These relations will be the spectroscopic modifications of the Pippard relations, as we have introduced for ammonium halides (NH_4Cl and NH_4Br) in our earlier studies /22,24/.

In order to derive the spectroscopic modifications of the Pippard relations, we start with the thermodynamic relation (Eq. 2.9). By substituting Eq. (2.6) into Eq. (2.9), we get

$$C_p = TV(\frac{dP_m}{dT})_m \alpha_p + TV\alpha_P V_c^{-1}\kappa_T^{-1}(\frac{dV_c}{dT}) + T(\frac{dS}{dT})_V \qquad (2.13)$$

In this expression, the second term on the right-hand side, which is equivalent to dP_m/dT by using the definitions of α_P and κ_T, vanishes since by definition the critical pressure is constant at the critical point. i.e., it is independent of temperature. Eq. (2.13) then becomes near the melting point in ammonia solid II

$$C_p = TV(\frac{dP_m}{dT})_m \alpha_p + T(\frac{dS}{dT})_m \qquad (2.14)$$

This is the first Pippard relation which relates the specific heat C_P to the thermal expansivity α_P near the melting point in the ammonia solid II. Similarly, the second Pippard relation relates the thermal expansivity α_P to the isothermal compressibility κ_T, which is given by

$$\alpha_p = (\frac{dP_m}{dT})_m \kappa_T + \frac{1}{V}(\frac{dV}{dT})_m \qquad (2.15)$$

near the melting point in ammonia solid II. In fact, this is the same expression given by Eq. (2.6), which has already been introduced by Pruzan *et al.* /15,16/ near the melting point for ammonia. We have also applied first (Eq. 2.14) and second (Eq. 2.15) Pippard relations to the ammonia solid I and II near the melting point in our earlier study /21/.

We can now relate the specific heat C_p to the Raman frequency shifts $\frac{1}{\nu}(\frac{\partial \nu}{\partial T})_P$ using the definition of the mode Grüneisen parameter γ_P (Eq. 2.10) in Eq. (2.14), which gives

$$C_p = -\frac{TV}{\gamma_P}(\frac{dP_m}{dT})_m \frac{1}{\nu}(\frac{\partial \nu}{\partial T})_P + T(\frac{dS}{dT})_m \qquad (2.16)$$

This represents a linear variation of the specific heat C_p with Raman frequency shifts $\frac{1}{\nu}(\frac{\partial \nu}{\partial T})_P$ near the melting point in ammonia solid II.

In this study we apply our spectroscopic modification of the first Pippard relation (Eq. 2.16) to the ammonia solid II near its melting point. For this application we use the Raman frequencies of the rotatory lattice (librational) mode of the ammonia solid II near the melting point.

3. CALCULATIONS AND RESULTS

In order to apply Eq.(2.16), we first calculated the volume of the ammonia solid II as a function of temperature for the fixed pressures of 3.65, 5.02 and 6.57 kbars using the experimental data due to Pruzan *et al.* /16/ according to Eq. (2.5). For this calculation we used the values of the volume parameters V_{II} and d_{II}, according to the empirical formula for the critical volume,

$$V_c(II) = V_{II} - d_{II}(T - T_{L-I-II}) \qquad (3.1)$$

and also the values of the critical exponent γ and amplitude k due to Pruzan *et al.* /16/, as we tabulate in Table 1. We also used for the V_s calculation the slope dP_m/dT whose values were obtained from the empirical relation

$$P_m(II) = 11.516[(\frac{T}{T_{L-I-II}})^{1.516} - 1] + 3.07 \qquad (3.2)$$

where the pressure is in the units of kbar. This then gives

$$dP_m(II)/dT = 4.999 \times 10^{-3} T^{0.516} \qquad (3.3)$$

due to Pruzan *et al.* /16/. We tabulate those values of dP_m/dT which were obtained experimentally according to Eq. (3.3) at the melting point ($T = T_m$) for the pressures of 3.65, 5.02 and 6.57 kbars in Table 2. We then calculated the Raman frequencies of the rotatory lattice (librational) mode in ammonia solid II near the melting point by means of Eq.(2.11).

As we have calculated in our previous study /19/, we first determined the coefficients a_0, a_1 and a_2 for $A(P)$ using the volume values and the Raman frequencies of the rotatory lattice (librational) mode at T = 224.1K and those at the melting point for the fixed pressures of 3.65, 5.02 and 6.57 kbars in ammonia solid II near the melting point due to Luo and Medina /14/. Those values of the volume and frequency at 224.1 K and those at the melting point are tabulated in Table 2. Those values of the coefficients a_0, a_1 and a_2 which we determined are tabulated in Table 1.

Using those values of a_0, a_1 and a_2, and also using the temperature dependence of volume due to Luo and Medina /14/, we were then able to calculate the Raman frequencies of this mode by Eq. (2.11). In this calculation we used the value of $\gamma_P = 0.9$ for the rotatory lattice (librational) mode, as given in Table 1. From the functional form of the Raman frequency, we evaluated the Raman frequency shifts as functions of temperature for three fixed pressures considered.

In order to establish a variation of the specific heat C_p with Raman frequency shifts $\frac{1}{\nu}(\frac{\partial \nu}{\partial T})_P$ according to Eq. (2.16), we also calculated the specific heat C_p for the ammonia solid II near the melting point. We first calculated the isothermal compressibility κ_T as functions of temperature for the fixed pressures of 3.65, 5.02 and 6.57 kbars for ammonia solid II near the melting point, according to Eq.(2.4). Similarly, we calculated the temperature dependence of the thermal expansivity α_p using Eq. (2.8) for those pressures studied. Then by

Table 1

Values of the triple temperature T_{L-I-II}, the volume parameters V_{II} and d_{II} (Eq. 3.1), the values of the critical exponent γ and the amplitude k (Eq. 2.1) for the ammonia solid II near the melting point due to Pruzan *et al.* /16/. The value of the isobaric mode Grüneisen parameter γ_p for the rotatory lattice (librational) mode due to Luo and Medina /14/ and values of the coefficients a_0, a_1 and a_2, which were calculated by means of Eq.(2.12), are also given here (see Ref. 19).

T_{L-I-II} (K)	$V_{II} \times 10^{-6}$ (m^3/mol)	$d_{II} \times 10^{-6}$ (m^3/mol)	γ	k	γ_p	$a_0 \times 10^{-2}$ (m^{-1})	$a_1 \times 10^{-2}$ (m^{-1}/kbar)	$a_2 \times 10^{-2}$ (m^{-1}/kbar^2)
217.34	21.13	0.0146	0.6 ±0.01	0.137	0.9	-43.6	17.4588	-1.4741

Table 2

Values of the molar volume and the Raman frequency of the rotatory lattice (librational) mode at the melting temperature T_m and at T = 224.1K in the ammonia solid II for the pressures indicated (see Ref. 19). The values of the slope dP_m/dT at the melting point, which were calculated using Eq.(2.16) and those obtained experimentally from Eq. (3.3), are also given here. The last column represents the values of the intercept $(dS/dT)_m$ (Eq.2.16).

P (kbar)	T_m (K)	$V_m \times 10^{-6}$ (m^3/mol)	$V_P \times 10^{-6}$ (m^3/mol) at 224.1K	ν_m $\times 10^{-2}$ (m^{-1})	$\nu_P \times 10^{-2}$ (m^{-1}) at244.1K	Calcul. dP_m/dT (bar/K)	Exper. dP_m/dT (bar/K)	$-(dS/dT)_m$ (J/mol.K^2)
3.65	225	20.82	20.81	267.4	268	74.85 ± 0.2	79.4	6.05
5.02	242	20.56	20.38	265.0	274	50.1 ± 0.2	82.4	1.16
6.57	260.3	20.27	19.96	266.8	278	54.9 ± 0.2	85.6	1.49

means of the thermodynamic relation (Eq. 2.9), we were able to calculate the specific heat C_p as functions of temperature for pressures of 3.65, 5.02 and 6.57 kbars for ammonia solid II near the melting point. Those values of C_p were obtained for the same temperatures as the Raman frequency shifts $\frac{1}{\nu}(\frac{\partial \nu}{\partial T})_P$ for the pressures studied. Within the same temperatures considered, we then plotted C_p against $\frac{1}{\nu}(\frac{\partial \nu}{\partial T})_P$ for the pressures of 3.65, 5.02 and 6.57 kbars, as shown in Figs. 1-3, respectively.

From those plots of C_p versus $\frac{1}{\nu}(\frac{\partial \nu}{\partial T})_P$, we deduced the values of dP_m/dT at the melting point for ammonia solid II for the three pressures studied, according to Eq. (2.13), where we used the value of the volume V_m at the melting temperature T_m. We present our calculated values of the slope dP_m/dT in Table 2 where we also give for comparison those experimental values of dP_m/dT which we obtained using the empirical formula (Eq. 3.3) with $T = T_m$ for the three pressures considered. Also, from our plots (Figs. 1-3) we deduced the values of $(dS/dT)_m$ at the melting point for the ammonia solid II. Those intercept values of $(dS/dT)_m$ are also given for the three pressures in Table 2.

As given in Figs. (1-3) and in Table 2, we also

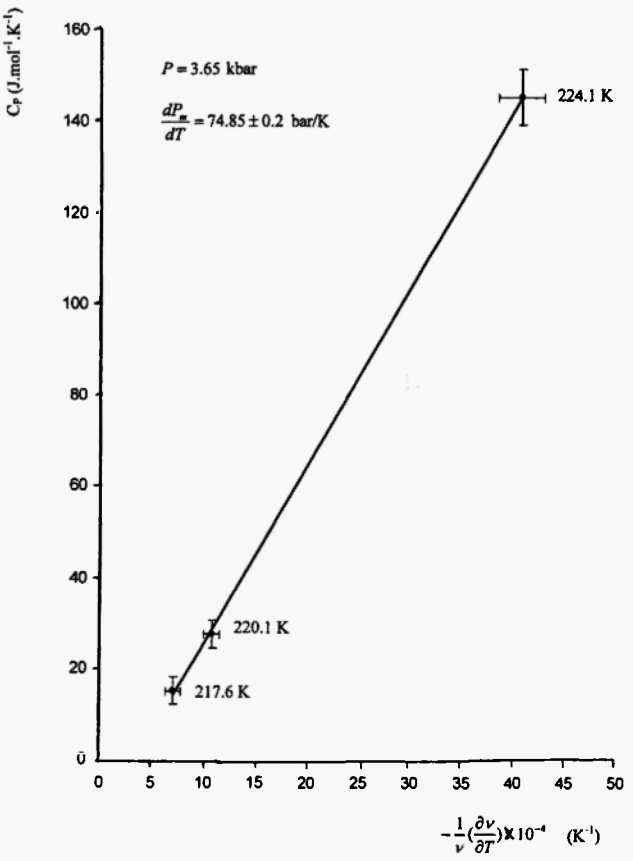

Fig.1: The specific heat C_p against the Raman frequency shifts $\frac{1}{\nu}(\frac{\partial \nu}{\partial T})_P$ of the rotatory lattice (librational) mode for the temperature indicated near the melting point in the ammonia solid II for the pressure of 3.65 kbar.

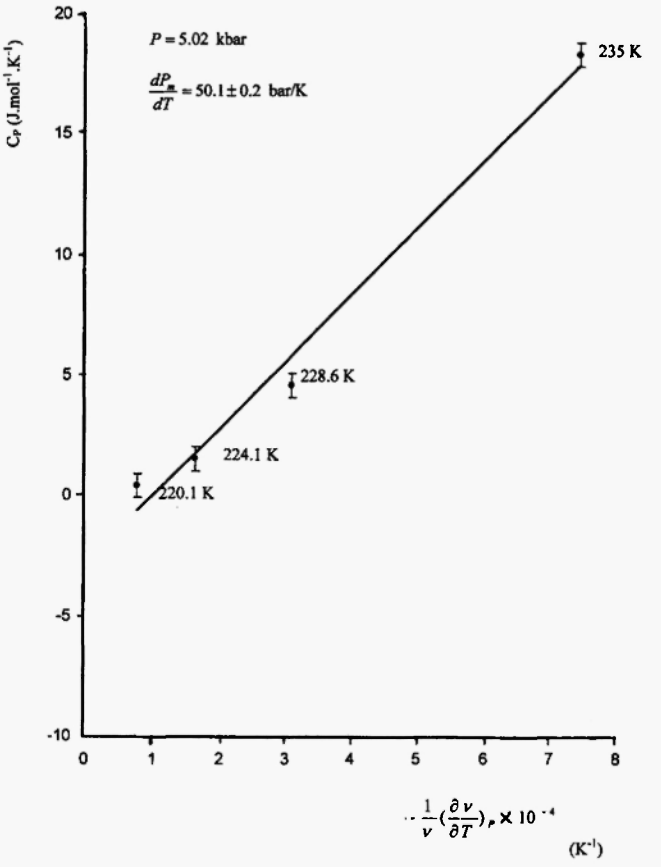

Fig.2: The specific heat C_p against the Raman frequency shifts $\frac{1}{\nu}(\frac{\partial \nu}{\partial T})_P$ of the rotatory lattice (librational) mode for the temperature indicated near the melting point in the ammonia solid II for the pressure of 5.02 kbar.

calculated uncertainties in dP_m/dT, due to those uncertainties in C_p and $\frac{1}{\nu}(\frac{\partial \nu}{\partial T})_P$, according to Eq. (2.16). Uncertainties in dP_m/dT were about ± 0.2 bar/K for the pressures of 3.65, 5.02 and 6.57 kbars in ammonia solid II.

Due to the uncertainties in the volume measurements $V_{II} = 21.13 \pm 0.02$ cm^3/mol and $d_{II} = 0.0146 \pm 0.0002$ cm^3/mol.K /16/, we first calculated uncertainties in V_c, according to Eq. (3.1). Since the critical exponent was obtained within the uncertainties $\gamma = 0.60 \pm 0.01$ /16/, we then calculated uncertainties in the isothermal compressibility κ_T using Eq. (2.4). This then led us to evaluate uncertainties in the specific heat $C_P - C_V$ by Eq. (2.9). Those uncertainties in the specific heat were calculated for the three pressures, namely, 3.65, 5.02 and 6.57 kbars in ammonia solid II.

We also needed to determine uncertainties in the frequency shifts $\frac{1}{\nu}(\frac{\partial \nu}{\partial T})_P$ for the pressures considered in ammonia solid II. For this calculation, we first calculated uncertainties in $\nu_P(T)$, according to Eq. (2.11). Since we calculated uncertainties in the crystal volume $V_P(T)$ from Eq. (2.5) by means of uncertainties in V_c (Eq. 3.1) and in γ, uncertainties in the rotatory lattice mode of $\nu_P(T)$ were then calculated (Eq. 2.11). This led us to evaluate uncertainties in $\frac{1}{\nu}(\frac{\partial \nu}{\partial T})_P$ for the

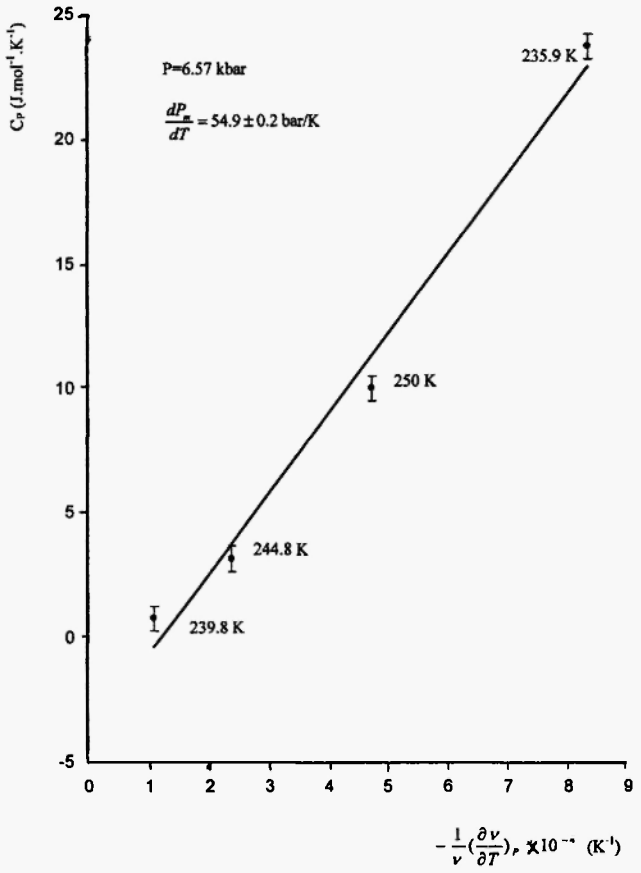

Fig.3: The specific heat C_p against the Raman frequency shifts $\frac{1}{\nu}(\frac{\partial \nu}{\partial T})_P$ of the rotatory lattice (librational) mode for the temperature indicated near the melting point in the ammonia solid II for the pressure of 6.57kbar

pressures of 3.65, 5.02 and 6.57 kbars in ammonia solid II.

Those uncertainties in C_p and in $\frac{1}{\nu}(\frac{\partial \nu}{\partial T})_P$ for the same temperatures are indicated for the three pressures studied in ammonia solid II in Figs. (1-3), respectively.

4. DISCUSSION

As seen from Figs. (1-3), we obtained a linear variation of the specific heat C_p with the Raman frequency shifts $\frac{1}{\nu}(\frac{\partial \nu}{\partial T})_P$ near the melting point in the ammonia solid II. This in fact verifies the spectroscopic modification of the first Pippard relation (Eq. 2.16) for ammonia solid II, as we have also verified the same relation for the ammonium halides (NH_4Cl and NH_4Br) near the λ point in our earlier studies /22,24/. Thus, by means of Eq. (2.16) the specific heat C_p can be estimated near the melting point for the ammonia solid II using the Raman frequency data. Since the Raman frequencies can be measured very accurately compared to the thermodynamic data, which are not easily obtained, Eq. (2.16) should be useful experimentally.

Regarding the values of the slope dP_m/dT, we see that our calculated value for P = 3.65 kbar is close to that obtained experimentally (see Table 2). Our calculated values of the slope dP_m/dT decrease as the pressure increases within the temperature regions considered. This contradicts the experimental values of dP_m/dT, which we obtained according to Eq. (3.3), that increase from 79 bar/K to 86 bar/K as the pressure increases (Table 2). The intercept values which we calculated using Eq. (2.16) also decrease as the pressure increases (Table 2). In particular, we find that for the pressure of 5.02 kbar our calculated values of dP_m/dT and dS/dT take on their minimum values. This is somehow unexpected since our calculated values of dP_m/dT do not follow the same trend as the experimentally obtained values. i.e. they do not increase as the pressure increases. Consequently, our intercept values of dS/dT for the pressures of 5.02 and 6.57 kbars, also follow the same trend as our values of dP_m/dT for this rotatory mode in ammonia solid II near the melting point.

Uncertainties in dP_m/dT were determined by calculating uncertainties in C_p and in $\frac{1}{\nu}(\frac{\partial \nu}{\partial T})_P$ according to Eq. (2.16), as given in Table 2 and Figs. (1-3). This uncertainty in dP_m/dT = ± 0.2 bar/K for the pressures of 3.65, 5.02 and 6.57 kbars is extremely small, because of the small uncertainties in C_p and in $\frac{1}{\nu}(\frac{\partial \nu}{\partial T})_P$. For P = 3.65 kbar (Fig. 1), uncertainties in C_p and in $\frac{1}{\nu}(\frac{\partial \nu}{\partial T})_P$ are comparatively larger as the melting temperature (T_m = 225 K) is approached, whereas for pressures of 5.02 kbar (Fig. 2) and 6.57 kbar (Fig. 3) uncertainties seem to increase as the temperatures are away from the melting temperatures.

The validity of the Pippard relations (Eqs. 2.14 and 2.15) is based on the assumption that the thermodynamic quantities, namely, the specific heat C_p, the thermal expansivity α_P and the isothermal compressibility κ_T exhibit similar critical behavior near the melting point. For the ammonia solid II, this also implies similar critical behaviour of C_p, α_P and κ_T near the melting point, as we have obtained for both ammonia solid I and II in our earlier study /21/. In this study we introduced the spectroscopic modification of the first Pippard relation (Eq. 2.16) whose validity is also based on similar critical behaviour of the specific heat C_p and the Raman frequency shifts $\frac{1}{\nu}(\frac{\partial \nu}{\partial T})_P$ near the melting point in the ammonia solid II. We also assumed that in the phase of the ammonia solid II, the value of the mode Grünesien parameter γ_P remains constant near the melting point for the three pressures of 3.65, 5.02 and 6.57 kbars (see Table 1). Considering this assumption, we conclude that the spectroscopic modification of the first Pippard relation (Eq. 2.16) is valid for the rotatory lattice (librational) mode of the ammonia solid II near the melting point.

5. CONCLUSIONS

We modified the Pippard relation spectroscopically using the Raman frequencies of the rotatory lattice (librational) mode in the ammonia solid II near the melting point. By plotting the specific heat C_p against the Raman frequency shifts $\frac{1}{\nu}(\frac{\partial \nu}{\partial T})_P$ of this mode for the temperatures considered close to the melting point, we obtained that C_p varies linearly with the $\frac{1}{\nu}(\frac{\partial \nu}{\partial T})_P$ for the three fixed pressures studied in the ammonia solid II. This enabled us to calculate the slope values of dP_m/dT which can be compared with those experimental values in this crystalline system.

REFERENCES

1. C.L. Nye and F.D. Medina, *Phys.Rev.***B32** 2510-2512 (1985).
2. R.L. Mills, D.H. Liebenberg and Ph. Pruzan, *J. Phys. Chem.* **86** 5219 (1982).
3. M. Gauther, Ph. Pruzan, J.M. Besson, G. Havel and G. Syfosse, *Physica B+C (Amsterdam)*, **139B** and **140B** 218-220 (1986).
4. R.C. Hanson and M. Jordan, *J. Phys. Chem.* **84** 1173- (1980).
5. S. Salihoglu, Ö. Tari and H. Yurtseven, *Phase Trans.* **72** 299-308 (2000).
6. Y. Enginer, S. Salihoğlu and H. Yurtseven, *Mat. Chem. Phys.* **73** 57-61 (2002).
7. R. Overstreet and W.F. Giaque, *J. Am. Chem. Soc.*, **59**, 254-258 (1937).
8. V.G. Manzhelii and A.M. Tolkachev, *Sov. Phys. Solid State*, **5**, 2506-2510 (1964).
9. V.G. Manzhelii and A.M. Tolkachev, *Sov. Phys. Solid State*, **8**, 827-830 (1966).
10. I. Olovsson and D.H. Templeton, *Acta. Cryst.* **12** 832- (1958).
11. J.W. Reed and P.M. Harris, *J. Chem. Phys.* **35** 1730- (1961).
12. J. Ekert, R. Mills and S. Satija, *J. Chem. Phys.* **81**, 6034- (1985).
13. R.K. Luo, C. Nye and F.D. Medina, *J. Chem. Phys.* **85** 4903-4904(1986).
14. R.K. Luo and F.D. Medina, *Phys.Rev.B*, **42** 3190-3193(1990).
15. Ph. Pruzan, D.H. Liebenberg and R.L. Mills, *J. Phys. Chem. Solids*, **47** 949-961 (1986).
16. Ph. Pruzan, D.H. Liebenberg and R.L. Mills, *Phys.Rev.Lett.* **48** 1200-1203 (1982).
17. H. Yurtseven, *J. Phys. Chem. A* **103** 5900-5904(1999).
18. H. Yurtseven, *Acta Physica Polonica. A* **99** 557-564(2001).
19. H. Yurtseven and S. Ugur, *Chin. J. Phys.* **41** 140-147(2003).
20. H. Yurtseven, *Chin. J. Phys.* **42** 209-217 (2004).
21. H.Yurtseven, *Int. J. Mod. Phys.* **B13** 2783-2790 (1999).
22. H. Yurtseven and W.F. Sherman, *J. Mol. Struc.* **323**, 243- 246 (1994).
23. H. Yurtseven and S. Salihoglu, *Chin. J. Phys.* **40** 416-423 (2002).
24. H. Yurtseven and W.F. Sherman, *J. Mol. Struc.*,**435**, 143- 150 (1997).